Implementation experiment of a honeycomb-backed MPP sound absorber in a meeting room

Hoshi, Kazuma ; Hanyu, Toshiki ; Okuzono, Takeshi ; Sakagami, Kimihiro ; Yairi, Motoki ; Harada, Shinji ; Takahashi, Seiji ; Ueda, Yasutaka

(Citation)
Applied Acoustics,157:107000

(Issue Date)
2020-01-01

(Resource Type)
journal article

(Version)
Accepted Manuscript

(URL)
https://hdl.handle.net/20.500.14094/90006344

Implementation experiment of a honeycomb-backed MPP sound absorber in a meeting room

Kazuma Hoshi[a], Toshiki Hanyu[a], Takeshi Okuzono[b], Kimihiro Sakagami[b], Motoki Yairi[c], Shinji Harada[d], Seiji Takahashi[d], Ueda Yasutaka[e]

[a]*Dept. of Architecture and Living Design, Junior College, Nihon University, 7-24-1, Narashinodai, Funabashi, 274-8501, Japan*
[b]*Environmental Acoustics Lab., Dept. of Architecture, Graduate School of Engineering, Kobe University, 1-1, Rokkodai, Nada, Kobe, 657-8501, Japan*
[c]*Kajima Technical Research Institute, 2-19-1, Tobitakyu, Chofu, 182-0036, Japan*
[d]*JSP Corporation Limited, 3-4-2, Marunouchi, Chiyoda, Tokyo, 100-0005, Japan*
[e]*Hazama Ando Corporation Limited, 515-1, Karima, Tsukuba, 305-0822, Japan*

Abstract

This paper presents the absorption performance of honeycomb-backed microperforated panel (MPP) absorbers, which are used to improve the acoustics of an existing meeting room where the reverberation time is too long for comfortable speech communication. In Japan, MPPs are difficult to use for interior walls owing to regulations. Therefore, we implemented the MPP absorber as an additional attachment that can be hung on walls and ceilings. First, the absorption characteristics of the MPP absorber were designed to reduce reverberation times at mid-frequency using an electroacoustical equivalent theory. Then, a wave-based finite element method simulation was used to determine the absorber placement. Reverberation absorption coefficients of the honeycomb-backed MPP absorber were also measured in an irregularly shaped reverberation chamber. Finally, the effect of the installed MPP absorbers was checked by acoustic parameter measurements. As a result, we observed that the reverberation time was reduced by half, the equivalent absorption area doubled, the early decay time values were also reduced, the clarity ($C_{50,\mathrm{mid}}$) increased by more than 5 dB, and the speech transmission index (STI) value increased by one rank.

Keywords: honeycomb-backed MPP, electroacoustical equivalent theory, finite element method, reverberation time. early decay time, speech transmission index.

1. Introduction

1.1. Backbround

A microperforated panel (MPP) is nowadays recognised as one of the most promising alternatives of next-generation sound absorbing material. Recently, many commercial products using MPPs have been produced and used in many countries, especially European countries. As is well known, an MPP was first proposed and its theoretical basis was studied by Maa [1, 2, 3, 4].

Email address: hoshi.kazuma@nihon-u.ac.jp (Kazuma Hoshi)

It is usually made of a thin panel (less than 1 mm thick) with submillimeter perforations at a perforation ratio of less than 1 %.An MPP is usually used as an interior surface with a rigid-back wall and an air cavity to produce Helmholtz resonators with each perforation and the air-back cavity.

In many cases, MPPs are thin and do not have enough strength. Thus, it is difficult to use them as interior walls, so they are often used for ceilings with lighting systems, etc. In addition, in Japan, MPPs are difficult to use for interior walls of buildings owing to the regulations required by the fire code. Considering this situation, Sakagami and Yairi and their collaborators proposed various types of space absorbers using MPPs [5, 6, 7] . At the same time, they proposed a honeycomb-backed MPP sound absorber and conducted theoretical and experimental studies[8, 9] . In the same study, the honeycomb was proven not only to strengthen the MPP enough for use as interior walls but also to improve its sound absorption performance.

The effect of a honeycomb backing or a partition in the cavity, which subdivides an air-back cavity, has been known for a long time and was applied mainly to porous materials [10]. This type of structure makes sound waves in the backing air cavity propagate normally to the absorber surface, which contributes to establishing a similar condition as a local reaction. In addition, as it subdivides the cavity so that the sound field is separate, the resonance characteristics are inferred to be enhanced.

Using a honeycomb backing, it is possible to produce a sound-absorbing panel with MPP, honeycomb, and a backplate that has enough strength and is used as a panel and not as an interior wall. This is an additional furniture-like panel attached from a ceiling or on a wall. This can be a practical method for applying MPPs to rooms without conflicting with regulations.

1.2. Purpose of this study

There are many implementation cases of MPPs in concert halls, public spaces and various buildings [11] . However, there are few examinations about the effect of MPPs' implementation with room acoustic parameters. Especially, the detailed examination of honeycomb backed MPP is not found, to the authors' best knowledge. Perforated materials are not allowed to use for interior walls in Japan, because there is the interior limitation by fire code and other related regulations. Therefore, to obtain best efficiency of a honeycomb backed MPP, it is set up a as detachable furniture, such as removable panel, etc. Furthermore, MPPs can be operated as detachable furniture and as sound absorbing parts in minimum area installation based on detailed numerical analysis, so that it is significantly effective for countermeasure of a shortage of sound absorption in existing buildings. In this study, we introduce detachable MPPs installation design technique based on detailed simulation and acoustic parameters' measurement.

1.3. Outline of implementation experiment

In this paper, the details of an implementation experiment of honeycomb-backed MPP absorbers for an existing meeting room to improve its acoustics will be reported. The meeting room has too-long reverberation times for speech communication, as will be discussed later. As mentioned, the above MPP is difficult to use as an interior wall owing to regulations in Japan. Therefore, to avoid conflict with the interior regulations, we manufactured an add-on honeycomb-backed MPP absorber that can be hung on walls and ceilings.

In this implementation project, the acoustical characteristics of the meeting room were first measured, and teams at Kobe University and Nihon University discussed methods for acoustics improvement using honeycomb-backed MPP absorbers with regard to design. Then, we determined the detailed the specifications of the MPP absorber and its installation location in the

room by using a theoretical analysis and a wave-based numerical simulation, respectively. The honeycomb-backed MPP absorber was produced by JSP Corporation. Hazama Ando Corporation made the experimental confirmation of the absorbers' acoustic performance and conducted the actual installation in the room.

2. Meeting room for experiment and specification formulation of absorbers

Figure 1 shows an interior view of the meeting room. The room is rectangular (3.55 m wide, 8.55 m depth and 3.00 m high), and its walls are hardly furnished with sound absorbing treatment. Its frequency characteristics of reverberation times measured according to ISO 3382-1 are shown in Figure 2. The reverberation time exceeds 2.0 s at frequencies from 250 Hz to 2 kHz. In particular, the values are over 2.5 s at 500 Hz and 1 kHz. This requires improvement for comfortable speech communication.

Figure 1: Experimental meeting room. Left: view from entrance to window. Right: view from window to entrance.

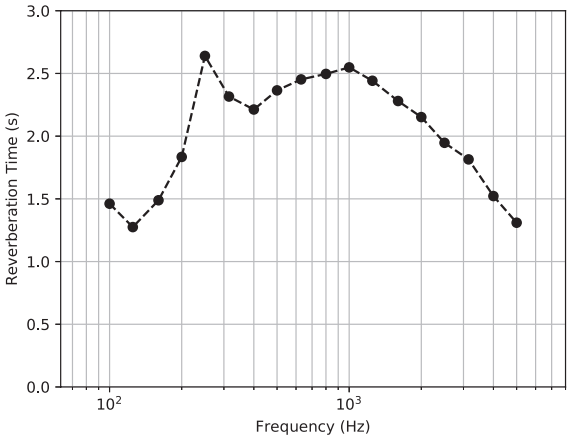

Figure 2: In-situ measurement values of reverberation time of meeting room (with no furniture).

The somewhat shorter reverberation times at lower frequencies might be owing to the sound transmission through the window and door inside the room. In this experiment, a frequency region important for speech communication was determined for the target of sound absorption treatment. Two honeycomb-backed MPP absorbers with different peak frequencies were used to control the reverberation times at mid-frequency, i.e. 500 Hz and 1 kHz. In addition, from a

design consideration, we explored the possibility of realising acoustical improvement with minimum furnishing of sound absorbers. Because it is not desirable to attach these absorbers at places where people using the room can reach, these absorbers were planned to be placed around the corners of ceilings and walls. Note that the effect of this absorber placement was evaluated on a preliminary basis using a wave-based numerical simulation, as will be presented in a subsequent section. Although honeycomb-backed MPP absorbers have enough strength, that absorber placement is important to avoid the unevenness of room surfaces from the perspectives of design and safety. Next, a honeycomb-backed MPP absorber was designed using an electroacoustical equivalent circuit theory. Based on the theory, the normalized surface impedance z_{n} of the honeycomb-backed MPP panel is calculated as

$$z_{\mathrm{n}} = \left(\frac{\rho_o c_o}{Z_{\mathrm{MPP}}} + \frac{\rho_o c_o}{j\omega M_{\mathrm{MPP}}} \right)^{-1} - j\cot(kL). \tag{1}$$

Here, the first term represents the transfer impedance of a limp MPP with the two parameters of the acoustic impedance of MPP Z_{MPP} and the surface density of MPP M_{MPP}. Maa ' s impedance model was used for Z_{MPP}. The characteristic impedance of air is represented as $\rho_o c_o$. j and ω represent the imaginary unit and angular frequency, respectively. The second term represents the normalized surface impedance of the locally reacting rigid-backed air cavity, which assumes that a sound wave propagates only perpendicularly to an MPP surface in the air cavity. The wave number in air and the air cavity depth are respectively represented as k and L in Eq. (1). The oblique incidence absorption coefficient α_θ and statistical absorption coefficient α_s are calculated respectively as

$$\alpha_\theta = \frac{4\mathrm{Re}[z_{\mathrm{n}}]\cos\theta}{(\mathrm{Re}[z_{\mathrm{n}}]\cos\theta + 1)^2 + (\mathrm{Im}[z_{\mathrm{n}}]\cos\theta)^2}, \tag{2}$$

$$\alpha_s = 2\int_0^{\pi/2} \alpha_\theta \sin\theta\cos\theta d\theta. \tag{3}$$

Here, the sound incidence angle is represented by θ. Considering the manufacturing cost of honeycomb-backed MPP absorbers, we determined the specifications of the absorbers. The material parameters of MPP are 0.5 mm in hole diameter, 1 mm in panel thickness, 0.785% in perforation ratio, and 1.13 kg/m^2 in surface density. Figure 3 shows the statistical absorption coefficient of the honeycomb-backed MPP absorber with the two air cavity depths of 10 mm and 50 mm, which were tuned to improve the acoustics at mid-frequency. The combination of two absorbers can effectively cover the target frequency range for the improvement of speech communication. For reference, the absorbers have a peak value in absorption at 548 Hz for L = 50 mm and at 1289 Hz for L = 10 mm.

3. Numerical simulation by frequency-domain finite element method

To confirm the absorption performance of the designed honeycomb-backed MPP absorbers in the installed condition, we performed preliminary numerical experiments using a dispersion reduced frequency-domain finite element method (FEM). The detailed formulation of the FEM and its performance over conventional FEM can be found in the literature [12, 13]. As shown in the literatures, the dispersion reduced FEM can be reduced the computational costs without reducing accuracy compared to conventional FEM. In the formulation, an MPP is assumed as a

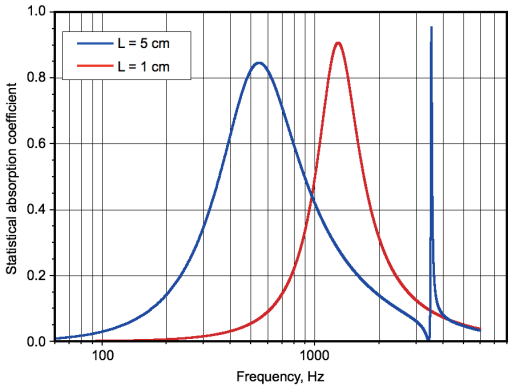

Figure 3: Statistical absorption coefficient of honeycomb-backed MPP absorbers with air cavity depths of 1 cm and 5 cm.

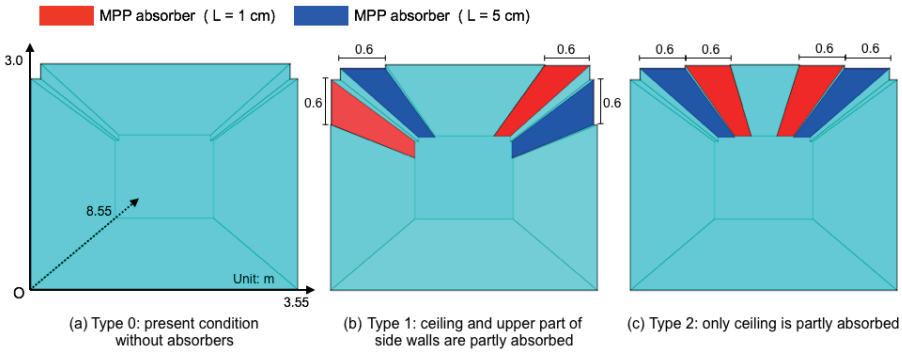

Figure 4: Two absorber arrangements including present condition without absorbers. (a) Type 0: present condition, (b) Type 1: ceiling and upper part of side walls are partly absorbed, and (c) Type 2: only ceiling is partly absorbed.

limp element, and the effect of micro-perforation is considered by Maa's well-known impedance model [2].

As mentioned in Sec. 2, we planned for the MPP absorbers to be placed on a ceiling and walls. Here, we investigated two absorber arrangements to confirm which is effective. In Type 1, the ceiling and the upper part of the side walls are partly absorbed. In Type 2, only the ceiling is partly absorbed. Figure 4(a)–(c) shows the two absorber arrangements, which include the present condition without absorbers, defined as Type 0. Note that the absorbers were not installed on walls with doors or windows owing to space limitations.

In the simulation, the room was modelled in a simple rectangular shape to keep computational costs within a manageable level and to avoid modelling complexity, as shown in Figure 1. Although the meeting room has a door, window, air conditioning system, sink cabinet, ducts, and steel braces for aseismic reinforcement, these were not modelled in the simulation.

In this section, we first present how to model honeycomb-backed MPP absorbers in FEM, in which the applicability of a simpler surface impedance model is compared with an exact extended reacting model. Then, the absorption performance of the two absorber arrangements, i.e. Type 1 and Type 2, are compared.

3.1. Modelling of honeycomb-backed MPP absorbers

Finite element analyses using a detailed model of honeycomb-backed MPP absorbers up to mid-frequency are still time-consuming because the detailed modelling of the honeycomb core complicates the finite element mesh and leads to a mesh with large degrees of freedom. As mentioned above, fortunately, the honeycomb-backed MPP absorbers might act as a locally reacting absorber when the cell size of the honeycomb core is small enough compared to the incident sound wavelength. In this case, absorber's properties can be characterized by a surface impedance on the absorber surface, and it is not necessary to model the honeycomb core in finite element meshes. This significantly reduces the computational cost of the finite element analyses. In this section, we test the applicability of the surface impedance model to the absorber by comparing it the exact extended reacting model. We performed two-dimensional sound field analyses with the two different reacting models. Figure 5 shows the analysed sound field with the two reacting models. In the extended reacting model, an MPP is modelled using limp MPP elements [12], and a honeycomb core is modelled using air elements and rigid partitions. By contrast, in the surface impedance model, the honeycomb-backed absorber is modelled as the surface impedance given by Eq. (1), which includes the reactance of the locally reacting rigid-backed air cavity. The material parameters of MPP used here are 0.5 mm in hole diameter, 0.5 mm in panel thickness, 0.785% in perforation ratio, and 0.6 kg/m^2 in surface density. In the analyses, the absorbers were installed on the ceiling and the upper part of the side walls, as shown in Figure 5. The air cavity depth of the absorber was 0.1 m. For the extended reacting model, the cell size and the thick of the partitions in the honeycomb core were, respectively, 4.9 cm and 1 mm. The sound pressure was calculated at frequencies from 88 Hz to 1414 Hz at 1 Hz intervals. Regarding the discretization of sound field, we used the dispersion reduced four-node quadrilateral elements [14] in air domain with sufficiently small size of elements, satisfying 24 elements per wavelength at the upper-limit frequency. Note that the detailed FE formulation used here can be found in the literature [12]. Figure 6(a) and (b) shows the 1/3 oct. band sound pressure level (SPL) distributions at 125 Hz, 250 Hz, 500 Hz, and 1 kHz in the two-dimensional room between the extended reacting model and the surface impedance model. At all frequencies, the SPL distributions of the surface impedance model approximate well the results of the extended reacting model. Figure 7 shows a comparison of frequency responses in the mean SPL over 20 receiving points between the extended reacting model and the surface impedance model. In addi-

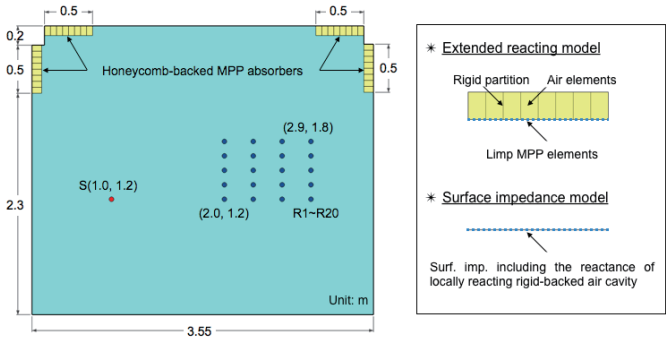

Figure 5: Two-dimensional sound field with honeycomb-backed MPP absorbers. Two absorber models called extended reacting model and surface impedance model are also shown: S and R1–R20 represent source position and 20 receiving positions.

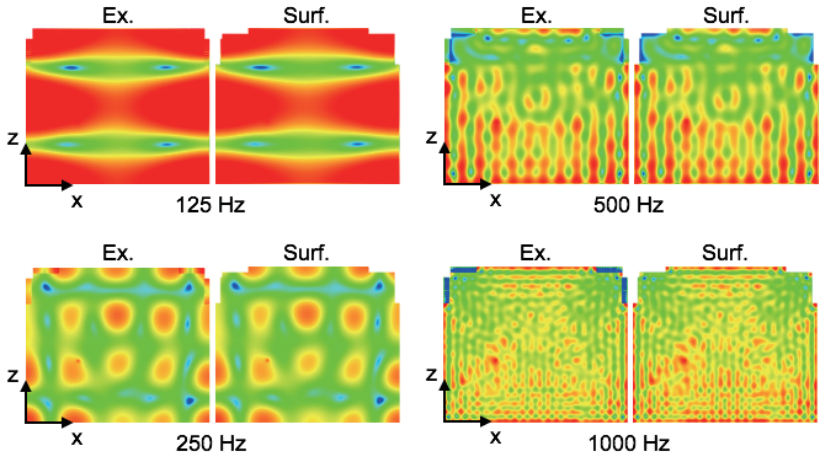

Figure 6: Comparison of 1/3 oct. band SPL distributions at 125 Hz, 250 Hz, 500 Hz, and 1 kHz between extended reacting model (Ex.) and surface impedance model (Surf.).

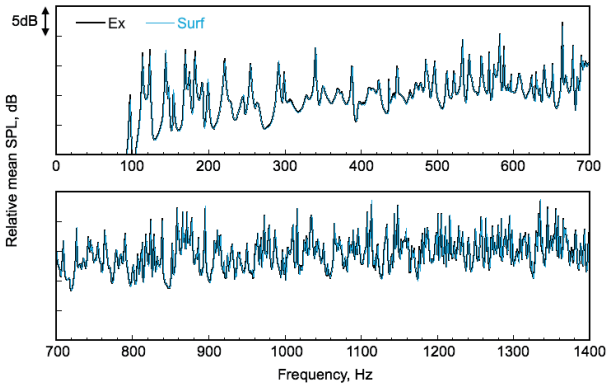

Figure 7: Comparison of frequency responses between extended reacting model (Ex.) and surface impedance model (Surf.).

tion, the surface impedance model captures well the results of the extended reacting model. The mean absolute difference over frequency between both models is 0.23 dB. These results indicate that the surface impedance of honeycomb-backed MPP absorbers is independent of the incident angles. According to the results, we used a simpler surface impedance model in Sec. 3.2.

3.2. Absorption performance of honeycomb-backed MPP absorbers

Using the three-dimensional frequency-domain finite element solver with the surface impedance model [13] , we compared the absorption performance of the two absorber arrangements as shown in Figure 4(b) and (c). The sound field in the present condition without the absorbers was also calculated. Figure 8 shows the source position and 12 receiver positions in the finite element analyses. Calculations were performed at mid-frequency (500 Hz and 1 kHz) at 0.5 Hz intervals. The reverberation time (T_{20}), the early decay time (EDT), and the clarity (C_{50}) were

calculated from the complex sound pressure. Note that an impulse response was calculated using an indirect approach with an inverse Fourier transform of the frequency response with IIR bandpass filtering. For reflecting boundaries, the real-valued surface impedance corresponding to statistical absorption coefficients of 0.059 and 0.057 was respectively given at 500 Hz and 1 kHz. These were estimated from a preliminary rough reverberation time measurement. The air domain was discretized using the dispersion reduced eight-node hexahedral elements [13]. The spatial resolution of resulting FE meshes satisfy 5 elements per wavelength at the upper-limit frequency and the meshes have approximately 850,000 degrees of freedom. Note that the degrees of freedom of FE meshes increase by 8 times when conventional eight-node hexahedral elements are used.

Figure 9 shows the reverberation time T_{20} for Type 0, Type 1, and Type 2. The figure also shows the reverberation time from the Eyring formula as a reference. Type 1 shows shorter reverberation times than Type 2, i.e. installing the absorbers into both the ceiling and the upper part of the side walls is more effective than only treating the ceiling. The reduction of $T_{20,\mathrm{mid}}$ (the averaged value of reverberation times at 500 Hz and 1 kHz) from Type 0 is, respectively, 19.2 % for Type 1 and 14.3 % for Type 2. Note that the FEM values are significantly longer than the ideal Eyring value. This is because the sound fields with absorbers become a non-diffuse sound field where bending of the decay curve occurs with unevenly distributed absorbers placement. On the other hand, with regard to the acoustical parameter corresponding to the perceived reverberance, Figure 10 shows $\mathrm{EDT}_{\mathrm{mid}}$ at 12 receiving positions among Type 0, Type 1, and Type 2. The values of $\mathrm{EDT}_{\mathrm{mid}}$ for Type 1 and 2 are significantly shorter than the T_{20} values. In addition, Type 1 shows shorter values than Type 2, in which the reduction of $\mathrm{EDT}_{\mathrm{mid}}$ averaged over 12 receiving points is 39.6 % for Type 1 and 34.9 % for Type 2. Furthermore, as the acoustical parameter corresponding to the clarity of speech, Figure 11 shows $C_{50,\mathrm{mid}}$ at 12 receiving points among Type 0, Type 1, and Type 2. It is observed that the increases in C_{50} by installing the absorbers are more than three times the just noticeable difference (JND) value of C_{50}, which is 1.1 dB [15]. Type 1 shows a 4.2 dB increase from the present condition, which is higher than that of Type 2 with a 3.4 dB increase. Based on the results of EDT and C_{50}, we expect an improvement in speech communication by the designed MPP absorbers, and we select the installation of the MPP absorbers into both the ceiling and side walls as the absorber arrangement. Note that since the meeting room has some scattering objects, e.g. the sink cabinet and the steel braces, the absorption effect of the MPP absorbers is actually more enhanced than in the numerical results.

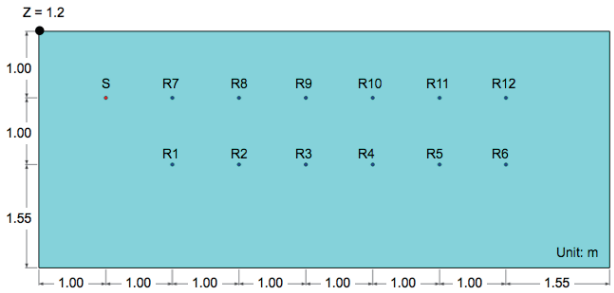

Figure 8: Source S and 12 receivers R1–R12 positions in finite element analyses.

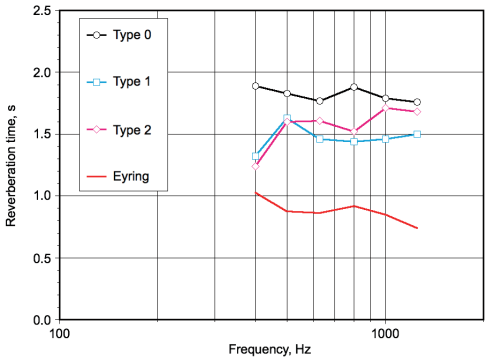

Figure 9: Reverberation times among Type 0, Type 1, and Type 2. Eyring value is also plotted as a reference.

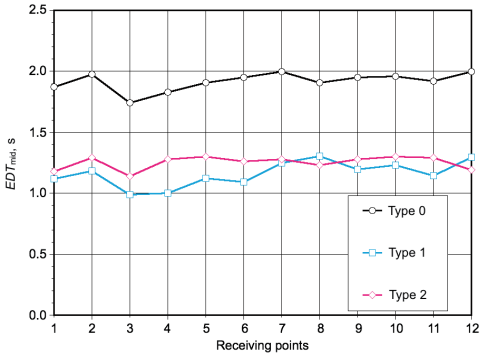

Figure 10: $\mathrm{EDT_{mid}}$ among Type 0, Type 1, and Type 2.

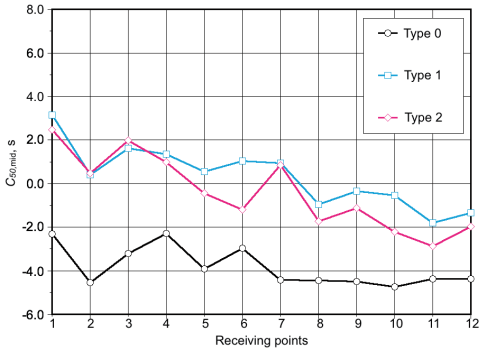

Figure 11: $C_{50,\mathrm{mid}}$ among Type 0, Type 1, and Type 2.

4. Production of honeycomb-backed MPP sound Absorbers and measurements of its absorption coefficients

The production of the honeycomb-backed MPP absorbers was carried out by JSP Corp. The finalised specifications of the absorbers are presented in Table 1, in which the perforation ratio is slightly modified from that of the preliminary investigation by considering the actual manufacturing process of perforated panels. Figure 12 shows the absorber that was produced. The absorber was assembled in a box-like shape of 500 × 600 mm with an MPP on the face and a blind (without an opening or perforation) panel on the back and sides. The internal honeycomb core had a square shape and 50 mm thick. All panels were made of polymethacrylstyrene sheet.

Then, the reverberation absorption coefficients of the manufactured honeycomb-backed MPP absorbers were measured in an irregularly shaped reverberation chamber at Hazama Ando Ltd. (V = 212 $\mathrm{m^3}$, floor area = 46 $\mathrm{m^2}$). The measurements were carried out according to JIS A 1409 (ISO 354 compatible). In the measurements, the area of the specimen was 9 $\mathrm{m^2}$, and the following cases were examined: (i) 50-mm-thick absorbers only and (ii) 10-mm-thick absorbers only. Figure 13 shows the results in comparison with the reverberation absorption coefficients of a fiberglass board (32 $\mathrm{kg/m^3}$) that was 25 mm thick as a reference.

From the results in cases (i) and (ii), the produced absorbers show an absorption peak at the frequencies that were theoretically predicted in the design stage. The absorption characteristics

Table 1: Specifications for produced honeycomb-backed MPP panels

Item			Specification
MPP base panel	Face	Base panel	Polymethacrylstyrene (MS) sheet: 1mm thick, 1.13 kg/m^2 area density
		Finishing	Colour matched with the wall and ceiling
	Frame/back		Polymethacrylstyrene (MS) sheet: 3 mm thick, 3.39 kg/m^2 area density
	Edge joints		Adhesion at the header
Perforation	Diameter		0.5 mm
	Ratio		0.77 %
	Pitch		5 mm
Honeycomb	Material		Polystyrene formed board: 1 mm thick, 0.275 kg/m^2 area density
	Shape		Lattice
	Pitch		50 mm square
	Install condition		No sticking on MPP base panel
Size (outside)			For low frequency: 500 mm $\times$ 600 mm $\times$ 54 mm (50 mm thick cavity)
			For high frequency: 500 mm $\times$ 600 mm $\times$ 14 mm (10 mm thick air cavity)

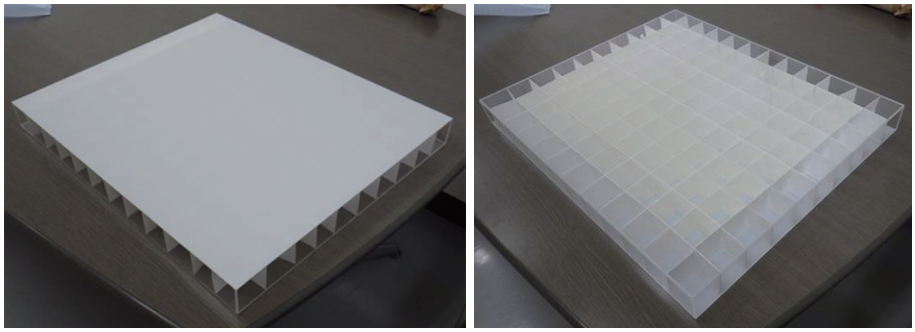

Figure 12: Example of produced honeycomb-backed MPP absorber. Left: Forward view. Right: Backward view.

are also as expected from the theoretical prediction. Therefore, we considered that they will obtain good results at the testing site as expected by the preliminary studies.

5. Implementation and measured results

Figure 14 shows the actual installation placement of the honeycomb-backed MPP absorbers in the meeting room. Photographs of the installed condition are presented in Figure 15. As the result of careful colour matching, the differences in the colours of the wall, ceiling, and absorbers are barely noticeable. Therefore, the absorbers are not distinguishable.

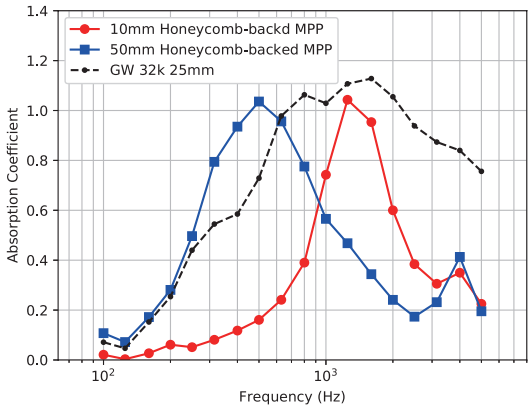

Figure 13: Measured absorption coefficient of produced honeycomb-backed MPP absorbers. For comparison, measurement values of glass wool of 32 kg/m^3 and 25-mm-thick density are also plotted.

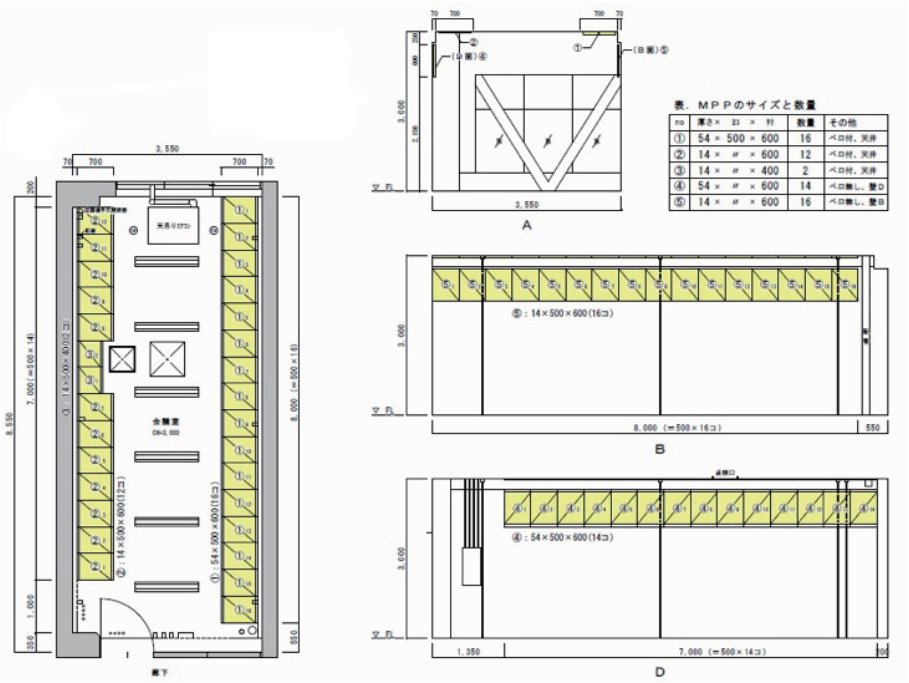

Figure 14: Install plan of honeycombed-backed MPP absorbers. Left: Installing position on ceiling board. Right: Installing position on both long side walls. Shown in each figure (1) and (4) are 50-mm-thickness panels; (2), (3), and (5) are 10-mm-thickness panels. Just one panel was unable to be installed for interfering with service duct.

Figure 15: Installation and arrangement of honeycomb-backed MPP absorbers.

5.1. Reverberation time measurement and its result

The reverberation time measurement after the implementation of the absorbers was conducted under the same conditions as the previous measurement. The measurement result shown in Figure 16 is plotted with the result before the installation. In addition, the equivalent absorption area calculated from the measurement results of the reverberation time is shown in Figure 17.

In Figure 16, the reverberation time from 200 Hz to 3 kHz is reduced significantly. In particular, the values from 500 Hz to 1 kHz are reduced by about half. This effect can also be seen in that the value of the equivalent area doubles, as shown in Figure 17. Only by using a small-area installment at the edge line of the ceiling and walls against all of the surface area, we were able to obtain a double equivalent absorption area using the honeycomb-backed MPP absorbers.

5.2. Results of EDT and C_{50}

The EDT and C_{50} values were also calculated from the impulse responses obtained by the reverberation time measurement. The calculation results of EDT and C_{50} are shown in Figures 18 and 19, respectively. In Figure 18, the EDT values from 250 Hz to 2 kHz are significantly reduced, especially at 500 Hz and 1 kHz. From these results, we expect that the reverberant is also significantly reduced. Second, in Figure 19, the C_{50} values at 500 Hz and 1 kHz increase significantly. Therefore, the $C_{50,mid}$ (average of the C_{50} values of 500 Hz and 1 kHz and five receiving points) values after and before installation are calculated. In the results, an improvement of more than 5 dB (–4.1 dB before installation and 1.5 dB after installation) can be seen by the effect of the MPP absorber installation. This result indicates that the clarity at midfrequency in each position in this meeting room can be improved.

5.3. STI measurement and results

We also conducted an impulse response measurement under actual meeting conditions for calculating the STI values [16] . Two conditions of a loudspeaker and receiving points were arranged. A loudspeaker simulated the directivity of actual people speaking in the room. The STI values in each condition are shown in Figure 20. The upper values are those after installation, and the lower ones are those before installation. The values after installation increase by more 0.1. The average STI values after installation and before installation are 0.67 and 0.55, respectively. This variant increases the rank from ‘fair’ to ‘good’. This result shows us that the speech environment of this meeting room can be improved significantly.

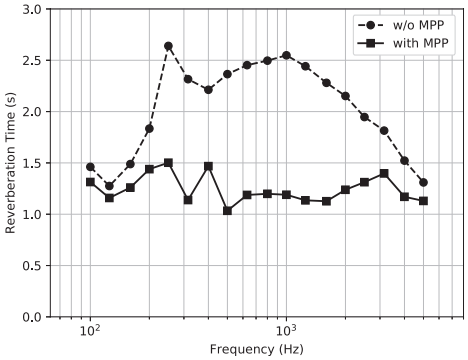

Figure 16: Reverberation time of meeting room with or without honeycomb-backed MPP absorbers (with no furniture).

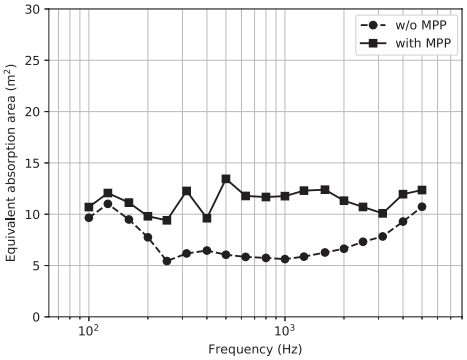

Figure 17: Equivalent sound absorption area of meeting room with and without honeycomb-backed MPP absorbers (with no furniture).

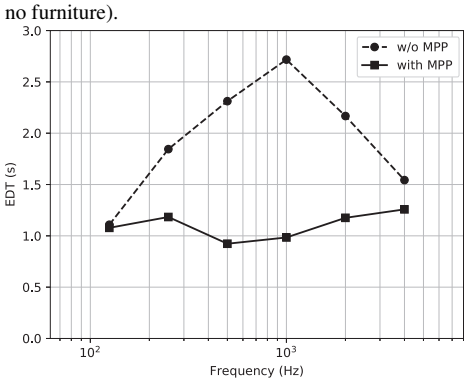

Figure 18: Early decay time (EDT) of meeting room with and without honeycomb-backed MPP absorbers (with no furniture).

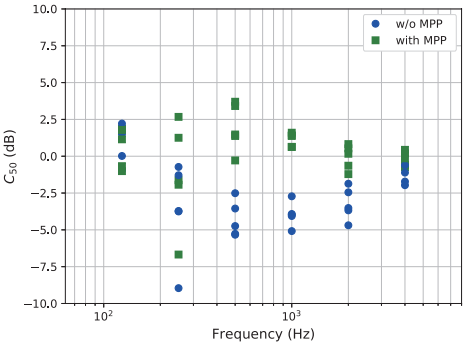

Figure 19: C_{50} in meeting room with and without honeycomb-backed MPP absorbers (with no furniture).

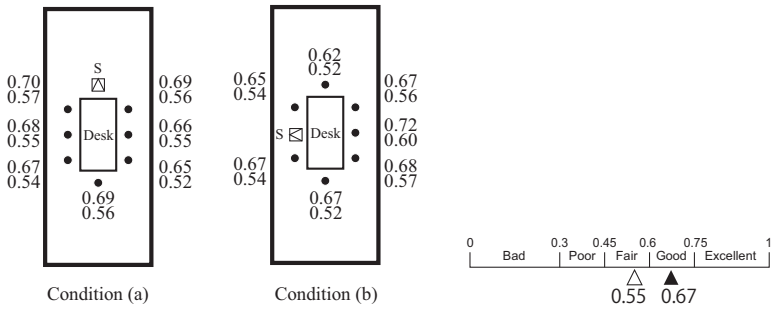

Figure 20: STI values of meeting room with or without honeycomb-backed MPP absorbers. S is sound source position. Upward values are measured before MPP absorber installation and downward values are measured afterward.

6. Conclusion

In this experiment, honeycomb-backed MPP absorbers were implemented in a small meeting room to improve the acoustics, and the absorption performance was examined. These MPP absorbers could be removed easily like furniture to comply with Japanese fire regulations. The absorption characteristics were designed using classical theory, an FEM simulation, and the measurement of the absorption coefficient in a reverberant chamber. In addition, the effect of the MPP absorber installation was checked by acoustic parameter measurement before and after installation.

In the present paper, we presented that the effectiveness of surface impedance model for the honeycomb-backed MPP absorbers in comparison with the exact extended reacting model. Then, the three-dimensional dispersion-reduced FEM with the surface impedance model was used to evaluate the acoustics in the meeting room with the two absorber's arrangements. Although room acoustic finite element simulations are one of the reliable methods based on wave acoustics theory, it is still time consuming when standard formulation of FEM and detailed absorber modelling are used for practical sized rooms to evaluate acoustical parameters derived from impulse responses. Therefore, the presented methodology would be beneficial to examine the effect of honeycomb-backed MPP absorbers installed inside practical sized rooms.

As a result, the reverberation time was reduced by half (in other words, the value of the equivalent absorption area doubled), the EDT values were also reduced, $C_{50,\mathrm{mid}}$ increased by more than 5 dB, and the STI value increased by one rank. This trial was also able to suggest that aiming acoustic effects could be obtained without drastic visual changes. An MPP absorber has significant potential in surface design. This trial suggests that MPP absorbers will become one of the most popular absorption techniques.

References

[1] Maa D.-Y. Theory and design of microperforated panel sound-absorbing constructions. Scientia Sinica. 1975;18:55–71.

[2] Maa D.-Y. Microperforated-panel wideband absorbers. Noise Control Eng J. 1987;29(3):77–84.

[3] Maa D.-Y. Potential of microperforated panel absorber. J Acoust Soc Am. 1998;104:2861–2866.

[4] Maa D.-Y. "Practical single MPP absorber", Int. J Acoust Vib. 2007;12:3–6.

[5] Sakagami K, Morimoto M, Koike W. A numerical study of double-leaf microperforated panel absorbers. Appl Acoust. 2006;67:609–619.

[6] Sakagami K, Nakamori T, Morimoto M, Yairi M. Double-leaf microperforated panel space absorbers: A revised theory and detailed analysis. Appl Acoust. 2009;70:703–709.

[7] Sakagami K, Oshitani T, Yairi M, E. Toyoda, Morimoto M. An experimental study on a cylindrical microperforated panel space sound absorber. Noise Control Eng J. 2012;60:22–29.

[8] Sakagami K, Yamashita I, Yairi M, Morimoto M. Sound absorption characteristics of a honeycomb-backed microperforated panel absorber: Revised theory and experimental validation. Noise Control Eng J. 2010;58(2):157–162.

[9] Yairi M, Minemura A, Sakagami K. Japan Patent Kokai 5008327; 2012.

[10] Ingard KU. Sheet absorbers. New York; 1994. Chap. 1 in Notes on.

[11] Adams T. Sound materials. Frame Publishers; 2016.

[12] Okuzono T, Sakagami K. A finite-element formulation for room acoustics simulation with microperforated panel sound absorbing structures: Verification with electro-acoustical equivalent circuit theory and wave theory. Applied Acoustics, 95. 2015;p. 20–26.

[13] Okuzono T, Sakagami K. A frequency domain finite element solver for acoustic simulations of 3D rooms with microperforated panel absorbers. Applied Acoustics, 129. 2018;p. 1–12.

[14] Guddati MN, Yue B. Modified integration rules for reducing dispersion error in finite element methods. Comput Methods Appl Mech Engrg. 2004;193:275–287.

[15] Bradley JS, Reich R, Norcross SG. A just noticeable difference in $C_5$0 for speech. Appl Acoust. 1999;58:99–108.

[16] Sound system equipment — Part 16: Objective rating of speech intelligibility by speech transmission index. Geneva, Switzerland; 2011.